

# Hydraulic safety margins and air-seeding thresholds in roots, trunks, branches and petioles of four northern hardwood trees

Jay W. Wason<sup>1</sup> , Katherine S. Anstreicher<sup>1</sup>, Nathan Stephansky<sup>2</sup>, Brett A. Huggett<sup>2</sup> and Craig R. Brodersen<sup>1</sup> 

<sup>1</sup>School of Forestry & Environmental Studies, Yale University, New Haven, CT 06511, USA; <sup>2</sup>Department of Biology, Bates College, Lewiston, ME 04240, USA

## Summary

Author for correspondence:

Jay W. Wason

Tel: +1 203 432 5151

Email: jay.wason@yale.edu

Received: 22 December 2017

Accepted: 28 February 2018

*New Phytologist* (2018) **219**: 77–88

doi: 10.1111/nph.15135

**Key words:** *Acer rubrum*, air-seeding threshold, embolism, *Fagus grandifolia*, *Fraxinus americana*, *Quercus rubra*, segmentation, xylem.

- During drought, xylem sap pressures can approach or exceed critical thresholds where gas embolisms form and propagate through the xylem network, leading to systemic hydraulic dysfunction. The vulnerability segmentation hypothesis (VSH) predicts that low-investment organs (e.g. leaf petioles) should be more vulnerable to embolism spread compared to high-investment, perennial organs (e.g. trunks, stems), as a means of mitigating embolism spread and excessive negative pressures in the perennial organs.
- We tested this hypothesis by measuring air-seeding thresholds using the single-vessel air-injection method and calculating hydraulic safety margins in four northern hardwood tree species of the northeastern United States, in both saplings and canopy height trees, and at five points along the soil–plant–atmosphere continuum.
- *Acer rubrum* was the most resistant to air-seeding and generally supported the VSH. However, *Fagus grandifolia*, *Fraxinus americana* and *Quercus rubra* showed little to no variation in air-seeding thresholds across organ types within each species.
- Leaf-petiole xylem operated at water potentials close to or exceeding their hydraulic safety margins in all species, whereas roots, trunks and stems of *A. rubrum*, *F. grandifolia* and *Q. rubra* operated within their safety margins, even during the third-driest summer in the last 100 yr.

## Introduction

The predicted rise in drought intensity and return frequency is expected to both reduce tree productivity and increase tree mortality (Choat *et al.*, 2012; Anderegg & Meinzer, 2015), which has been mechanistically linked to hydraulic failure of the xylem network and commensurate loss of water supply to the canopy (Brodrigg & Cochard, 2009; Allen *et al.*, 2010; Choat *et al.*, 2012; Urli *et al.*, 2013; Adams *et al.*, 2017). Hydraulic failure arises due to the inherent metastability of xylem sap as it moves through a complex network of conduits under negative pressure (Dixon & Joly, 1895; Zimmermann, 1983). The xylem conduits are therefore vulnerable to the formation of gas embolisms that block water transport (Tyree & Sperry, 1989).

Xylem network vulnerability to systemic embolism spread should then be based on the frequency and distribution of interconduit connections, and the resistance of the pit membranes therein, to the movement of air between conduits. This resistance is typically characterized as the negative pressure required to pull gas into an adjacent water-filled conduit across the pit membrane ('air-seeding threshold'; Zimmermann, 1983). That pressure threshold is thought to be determined by the effective pore radius along the tortuous pathway through the pit membrane, where the pore radius determines the pressure differential supported by the air–water interface (i.e. meniscus) according to the Young–

Laplace equation, although the exact mechanisms are still unclear. Thus, the same pathway that increases xylem network redundancy by providing alternate pathways for water flow also can facilitate the spread of air embolisms that render the network dysfunctional. Xylem-network connectivity, interconduit air-seeding pressures, and the spatial distribution of air in the network are predicted to be the major factors driving the shape of xylem vulnerability curves. Although xylem-network connectivity determines where embolisms spread in the network (Loepfe *et al.*, 2007; Mencuccini *et al.*, 2010; Brodersen *et al.*, 2011; Lee *et al.*, 2013), the air-seeding threshold of pit membranes provides information about when embolisms begin to spread during drought conditions (cf. 'air-entry point'; Meinzer & McCulloh, 2013).

To date, the single-vessel air-seeding threshold of intervessel pit membrane connections has been studied in relatively few vessel-bearing species (Melcher *et al.*, 2003; Choat *et al.*, 2004, 2005; Jansen *et al.*, 2009; Christman *et al.*, 2012; Johnson *et al.*, 2014; Pratt *et al.*, 2015; Venturas *et al.*, 2016); however, the air-seeding threshold often appears to be a variable trait. In our evaluation of published air-seeding data, most studies report that 40–50% of vessels within an organ embolize before pressures reach  $-1$  MPa, with a maximum of *c.* 80% (Pratt *et al.*, 2015). Meanwhile, the remaining vessels in the same organ were highly resistant, with air-seeding values ranging from  $-1$  to  $-5$  MPa. By contrast, *Acer saccharum* air-seeding thresholds have been

shown to have less variability within an organ (e.g. petioles, stems, trunks, roots) than other species, and *A. saccharum* shows consistent mean differences in air-seeding threshold when comparing across organs (Melcher *et al.*, 2003; Choat *et al.*, 2005). Therefore, it is uncertain how air-seeding thresholds, an important driver of drought resistance and the shape of xylem vulnerability curves, vary within and across species and plant organs.

The vulnerability segmentation hypothesis (VSH; Tyree & Zimmermann, 2002) predicts that xylem in low-cost, distal organs (e.g. leaves and fine roots) should be more vulnerable to embolism spread than xylem in higher-cost organs (e.g. trunks and stems). When constructed this way, embolism spread in leaves would stop water loss and protect the more permanent, high-investment organs from increasingly negative xylem sap pressures (Zimmermann, 1983; Tyree *et al.*, 1993; Tsuda & Tyree, 1997; Tyree & Zimmermann, 2002; Johnson *et al.*, 2016). However, as plants transpire, xylem sap potentials become more negative with increasing distance from the soil. Therefore, a hypothetical plant constructed with equal air-seeding thresholds in all organ types (i.e. not constructed following the VSH) would still be expected to have embolisms first form and spread in organs experiencing the most negative water potentials – leaf xylem. Studies have found evidence for (Tsuda & Tyree, 1997; Choat *et al.*, 2005; Bucci *et al.*, 2012; Charrier *et al.*, 2016; Hochberg *et al.*, 2016; Johnson *et al.*, 2016) and against (Cochard *et al.*, 1992; Hao *et al.*, 2013; Bouche *et al.*, 2016; Skelton *et al.*, 2017) the VSH, suggesting it may not be an universal strategy across species (Hacke & Sauter, 1996; Brodersen, 2016; Zhu *et al.*, 2016).

Although the air-seeding threshold of xylem vessels is important, it is most relevant to plant productivity and survival within the broader context of the xylem pressures that plants experience in the field (Choat *et al.*, 2012; Delzon & Cochard, 2014). The 'hydraulic safety margin', defined as the most negative water potential experienced by plants minus the water potential leading to significant hydraulic failure, provides a metric of how close plants are to hydraulic failure in the field (Meinzer *et al.*, 2009). Importantly, increasing the air-seeding threshold of a specific organ via more resistant or fewer pit membranes may come with an associated cost of reduced hydraulic conductivity, although it remains unclear how strong this trade-off is in woody plants (Gleason *et al.*, 2016). Furthermore, vulnerability curves and safety margins are most commonly available for branches, whereas data for leaves, petioles, trunks and roots are less common. Understanding air-seeding thresholds and safety margins in organs with different biomechanical roles is critical for understanding what trade-offs and selective pressures exist in the construction of the xylem of woody plants.

The goal of this study was to measure the air-seeding thresholds of roots, trunks, branches and petioles along with the mid-day water potentials experienced by those organs to (1) determine if the VSH is supported and (2) establish hydraulic safety margins for two ring-porous and two diffuse-porous tree species in the northeastern United States. Single-vessel air-seeding thresholds were then compared to points from benchtop dry-down vulnerability curves in current-year stems to determine

how the air-seeding thresholds relate to whole-organ vulnerability. Single-vessel air-seeding thresholds of sapling and canopy height trees also were compared to evaluate the influence of different hydraulic demands of trees at two life-history stages. We then compared single-vessel air-seeding thresholds across organ types as well as across growth rings in perennial organs. This experiment coincided with the third driest summer in the past 100 yr at the study site (Supporting Information Fig. S1), thereby providing additional context about how close these four hardwood species were pushed to their physiological tipping point.

## Materials and Methods

### Plant material

All measurements were made on forest-grown sapling (mean diameter =  $1.3 \pm 0.3$  cm and age =  $16 \pm 6$  yr at 20 cm above soil surface) and canopy (mean diameter =  $38 \pm 16$  cm and age =  $79 \pm 16$  yr at breast height) sized trees of *Acer rubrum* L., *Fagus grandifolia* Ehrh., *Fraxinus americana* L. and *Quercus rubra* L. at Harvard Forest, Petersham, MA, USA. Single-vessel air-seeding measurements were conducted in June, July and August of 2016 on three understory sapling trees and two to three canopy trees of each species following the methods of Melcher *et al.* (2003) and Johnson *et al.* (2014). Entire saplings were excavated, including roots, placed in black plastic bags with moist paper towels, and transported to the laboratory within 15 min. Bagged saplings were kept moist and stored at 4°C while organ samples were excised for measurement. Saplings were collected from areas of similar shade and soil conditions and all measurements were completed within 36 h. On each sapling, the air-seeding threshold was measured on six samples each of petioles ( $1.5 \pm 0.3$  mm; mean diameter  $\pm$  SD), current-year stems ( $2.1 \pm 0.7$  mm), multi-year stems (3-yr old;  $4.4 \pm 1.2$  mm), trunk samples (30–50 cm above soil surface;  $11.7 \pm 3.6$  mm) and roots (> 20 cm from the tree base;  $3.6 \pm 1.1$  mm).

Sampling of canopy-tree organs required some variation in protocol. Petiole ( $1.5 \pm 0.3$  mm; mean diameter  $\pm$  SD), current-year ( $3.1 \pm 1.1$  mm) and multi-year stem samples ( $6.1 \pm 1.5$  mm) were collected from one or two sun-exposed branches in the upper canopy of each tree (c. 20 m above the forest floor) using a canopy lift (Scanlift SL240, Joensuu, Finland). Branches were transported to the laboratory and processed identically to the saplings. In addition, trunk and root samples of canopy trees were collected using a 5/8-inch inner-diameter plug cutter (Steelex D1050 Tenon Cutter, Woodstock International Inc., Bellingham, WA, USA) and power drill. Due to the destructive nature of this sampling, only one to two 'plugs' were collected from each tree's trunk and roots until six measurements could be made within the 2016, 2015 and 2014 growth rings (three measurements in earlywood and three measurements in latewood for trunks). Plugs were stored in plastic bags with moist paper towels and transported back to the lab for immediate measurements. The upper surface of each plug was shaved with a microtome (Gärtner *et al.*, 2014) to provide a flat surface for air-seeding measurements. *Fraxinus americana* and *Q. rubra* trunks can have

long vessels resulting in a low number of vessel endings within each plug. Therefore, trunk sampling was modified for these two species to collect longer samples and increase the chances of encountering a vessel ending during sampling. A section of trunk xylem and bark was chiseled out that was *c.* 10 cm wide, 30 cm tall and 5 cm deep. The upper and lower surfaces of the section were shaved clean with a sharp knife and air-seeding measurements progressed identically to that of the plugs.

Long samples may result in multiple vessels needing to air-seed before detection with the single-vessel air-injection method (Venturas *et al.*, 2016). Therefore, and to facilitate comparisons across organ types and species, most samples were 6 cm long unless otherwise noted, thereby balancing sampling efficiency and still maintaining a relatively short sample length (as suggested by Venturas *et al.*, 2016). Some samples were necessarily shorter, for example *F. grandifolia* and *Q. rubrum* petioles, which had a maximum length of *c.* 1–3 cm, as well as all canopy-sized tree root ‘plugs’ and *A. rubrum* and *F. grandifolia* trunk ‘plugs’ that were *c.* 1.5 cm. To assess the potential impact of sample length when comparing air-seeding measurements across organs for each species (Venturas *et al.*, 2016), we recorded and report the number of open vessels (vessels without an ending in the segment; see next section) that were encountered during sampling.

### Single-vessel air-seeding threshold

In order to measure the vulnerability to air-seeding of pit-membranes between two adjacent vessels we used the single-vessel air-injection method (Melcher *et al.*, 2003; Johnson *et al.*, 2014). Trees were processed starting with petioles, followed by stems, multi-year stems, trunks and then roots. Extensive drying of pit membranes could reduce resistance to air-seeding due to pit membrane shrinkage (Zhang *et al.*, 2017). Therefore, in addition to storing saplings whole in a bag at 4°C with moist paper towels during sampling, measurements proceeded rapidly from the time of excision. Briefly, samples were excised in the air, cut to length with a razor blade and mounted in a multi-position vice (Panavise model 201, Medford, OR, USA). The proximal end of the sample was immediately immersed in water more than half the length of the sample and the transverse surface of the sample (distal end) was observed under a dissecting microscope to identify a vessel for measurement. Next, a glass capillary tube (WPI, 1B150-4; WPI Inc., Sarasota, FL, USA) that had been pulled to a tip *c.* 15–20 µm in diameter (Vertical Micropipette Puller, model P-30; Sutter Instrument, Novato, CA, USA) was inserted into a xylem vessel using a micromanipulator, and glued in place with a cyanoacrylate glue (Loctite 409; Loctite, Düsseldorf, Germany) and a hardening accelerant (Loctite 712). The end of the capillary tube was attached to a 1-m length of PEEK tubing (51085K48; McMaster-CARR, Princeton, NJ, USA) connected to a Scholander pressure chamber (#1505; PMS Instruments, Corvallis, OR, USA). Working with the samples in this way minimized exposure to air and kept samples hydrated and as close to their natural state as possible. Pressure was increased at a rate of *c.* 0.5 MPa min<sup>-1</sup> (Johnson *et al.*, 2014) until bubbles were visible exiting the submerged proximal end of the sample. This positive

pressure value was recorded as equal to but opposite the sign of the air-seeding threshold of the aspirated pit membrane of the vessel. Measurements more negative than -5.5 MPa were terminated at that point for safety and those measurements were discarded. Measurements less negative than -0.05 MPa also were discarded because the vessel was presumed to be open at both ends of the sample (Johnson *et al.*, 2014). Each petiole, current-year stem and root sample was used to make a single air-seeding measurement. The six multi-year stem and six trunk samples were each randomly split to sample early-wood or late-wood vessels. On each of these samples, three air-seeding measurements were made in random order – one each in vessels of the 2016, 2015 and 2014 growth rings – at *c.* 120 degree intervals around the stem sample to avoid any artifacts resulting from previous measurements on the same sample. To determine if air-seeding threshold varied across organ types and size classes, air-seeding threshold (log transformed) was modeled as a function of organ type interacting with size class for each species using linear-mixed-effects models in R (R Core Team, 2015; Bates *et al.*, 2016). Models included a random intercept for organ sample within tree to account for the nested sampling design. Tukey’s pairwise comparisons were used to determine significant differences in air-seeding threshold between each organ type and size-class combination for each species ( $\alpha = 0.05$ ). To test whether air-seeding threshold differed between early- and latewood vessels, air-seeding threshold (log-transformed) was modeled as a function of wood type (early or late) interacting with species with a random intercept for growth ring nested within organ sample and tree.

In order to determine if air-seeding threshold changed with xylem age, the slope of a regression between the air-seeding threshold (MPa) and xylem age (ages of 0, 1 and 2 for vessels formed in 2016, 2015 and 2014, respectively) was calculated for each multi-year and trunk sample. A positive slope indicated that air-seeding threshold became less negative with age in that sample (i.e. resistance to air-seeding decayed with time). Slopes were averaged by species and size class and each group’s slope was tested against zero with Bonferroni corrected one-sample *t*-tests ( $\alpha = 0.05$ ). We repeated this analysis to test if the glue accelerant, or time since excision, impacted measurements by replacing ‘xylem age’ with ‘measurement order’ and found that there was no effect of measurement order on air-seeding threshold.

### Benchmark dry-down vulnerability curves

Single-vessel air-seeding threshold data were compared to organ-level percentage loss of conductivity (PLC) curves for current-year stems in saplings of each species using the benchmark dry-down method (cf. Choat *et al.*, 2010). Branches 1–2 m long (one branch per tree) were collected in August 2017 during predawn hours, stored in black plastic bags with moist paper towels, and transported to the lab. A segment of each branch containing only current-year’s extension growth was labeled for measurement. Branches were then placed on the laboratory bench at room temperature and allowed to dry to a range of water potentials for up to 72 h before being returned to black plastic bags for a

minimum of 30 min to equilibrate. Water potential was measured on 1–2 leaves using a pressure chamber. Then, the cut end of the branch was submerged in water and recut with shears three to five times in *c.* 1 cm increments and the branch was covered in a black plastic bag to prevent transpiration and facilitate relaxation of water tension (Wheeler *et al.*, 2013; Torres-Ruiz *et al.*, 2015). Branches were relaxed for between 10 and 30 min depending on the water potential (longer times for more negative water potentials).

Following relaxation, the branch was progressively cut underwater with shears, until only the labeled current-year segment remained. Segment ends were trimmed under water with a fresh razor blade before measurements. The segment was then attached to a modified Sperry apparatus (Sperry *et al.*, 1988) equipped with a flow meter (SLI-0430; Sensirion, Stäfa, Switzerland) and filled with filtered and degassed 20 mM KCl solution. Native conductivity ( $K_{\text{nat}}$ ) was measured on each segment using a constant pressure head for each sample of 1–6 kPa. Segments were then vacuum-infiltrated (Espino & Schenk, 2011) overnight to remove embolisms. The next day, segment ends were trimmed underwater with a fresh razor blade and maximum conductivity ( $K_{\text{max}}$ ) was measured. PLC was calculated as  $(1 - (K_{\text{nat}}/K_{\text{max}})) \times 100$ . PLC curves were fit with Weibull curves and bootstrapped 95% confidence intervals  $P_{12}$ ,  $P_{25}$  and  $P_{50}$  were extracted using the FITPLC package in R (Duursma & Choat, 2017) to compare with air-seeding threshold data.

### Vessel diameter

In order to determine if air-seeding threshold was correlated with vessel size, the mean vessel-lumen diameter was calculated for each species and organ type by using two or three cross-sections per organ collected from the same plant material used for air-seeding. Cross-sections were stained with a mixture of Astra blue and Safranin-O (van der Werf *et al.*, 2007) and imaged between 1× and 10× with a compound microscope (Leica ICC50 HD; Leica Microsystems, Buffalo Grove, IL, USA). Images were processed in IMAGEJ software (National Institutes of Health) to isolate individual vessels in binary images and to automatically calculate the lumen area of each vessel. Vessel-lumen areas were converted to vessel-lumen diameters by assuming circularity. Vessel-lumen diameter was log-transformed and differences in the mean vessel-lumen diameter across organs were tested using ANOVA and Tukey's pairwise comparisons for each species and size class. Additionally, the mean air-seeding threshold of each organ type was regressed against mean vessel-lumen diameter of each organ type for each species and size class using major axis regression in R (Warton *et al.*, 2014).

### Plant organ water potential

In order to determine water-potential gradients in trees, midday water potentials (between 13:00 h and 15:00 h) were measured on two individuals of each species and size class. Canopy trees used were the same as those sampled for air-seeding threshold (above). Due to the destructive nature of sampling saplings,

different individuals of similar age and size from nearby areas were used for sapling water potentials. Thermocouple psychrometers (JRD Merrill Specialty Equipment, Logan, UT, USA) were used to measure water potential because standard pressure-chamber methods are not possible for all organ types (i.e. stems, trunks and roots). Petiole, current-year and multi-year stem segments *c.* 1 cm long were excised from the intact plant and immediately sealed in individual psychrometer chambers (JRD Merrill Specialty Equipment, Part #83-500). Trunk samples were collected using a 35-mm-long Trephor microcorer (Rossi *et al.*, 2006) at 30 cm above the soil surface for saplings or at breast height for canopy trees. Root samples from canopy trees were collected at > 20 cm along a main root from the base of the tree using the microcorer. Root samples from sapling trees were collected > 20 cm along main roots from the base of the tree but were of narrow enough diameter to be excised into *c.* 1-cm-long segments and placed in the psychrometer chamber. Psychrometer chambers (#83-3V and 81-500; JRD Merrill Specialty Equipment, Logan, UT, USA) containing samples were connected to a data logger (Campbell CR6; Campbell Scientific Inc., Logan, UT, USA) with a multiplexer. The chambers were bagged and suspended in a circulating water bath held at a constant  $25 \pm 0.2^\circ\text{C}$  and allowed to equilibrate for 6–8 h until water-potential readings stabilized. All psychrometers were calibrated between 0 and  $-7.1$  MPa using NaCl solutions ( $R^2 = 0.96 \pm 0.03$  (mean  $\pm$  SD); Brown & Bartos, 1982). Psychrometers have been used to verify that pressure chamber measurements are accurate (Boyer, 1967); we confirmed this with a separate experiment that compared psychrometer and pressure chamber measurements (Fig. S2). To verify that tree water potentials relaxed at night, we also measured predawn (between 04:00 h and 05:00 h) and midday (between 13:00 h and 15:00 h) water potentials with a pressure chamber (Scholander *et al.*, 1965) on 8–12 leaves per species and size class. All analyses, statistics and figures were conducted or produced in R (R Core Team, 2015; Wickham & Chang, 2016).

## Results

Only canopy *A. rubrum* trees exhibited single-vessel air-seeding thresholds consistent with the VSH: petiole ( $-0.8 \pm 0.4$  MPa; mean air-seeding threshold  $\pm 2$  SE) and root ( $-0.6 \pm 0.3$  MPa) air-seeding thresholds were both significantly less negative than multi-year stems ( $-3.0 \pm 0.8$  MPa;  $\alpha = 0.05$ ; Fig. 1a). By contrast, the other diffuse porous species, *F. grandifolia*, and the two ring-porous species, *F. americana* and *Q. rubra*, did not exhibit evidence for segmentation of air-seeding thresholds in either canopy trees or saplings (Fig. 1b–d). Although there was not a consistent mean difference, three species had organs where the air-seeding threshold measurements in one size class were less resistant than the mean value of the other size class. For example, all measurements in roots from canopy-size *A. rubrum* ( $-0.6 \pm 0.3$  MPa; mean air-seeding threshold  $\pm 2$  SE) and *Q. rubra* ( $-0.5 \pm 0.2$  MPa) were less resistant the mean value for their sapling roots (*A. rubrum*:  $-1.9 \pm 0.7$  MPa; *Q. rubra*:  $-1.5 \pm 0.5$  MPa; Fig. 1a,d), and sapling petioles in *F. grandifolia*

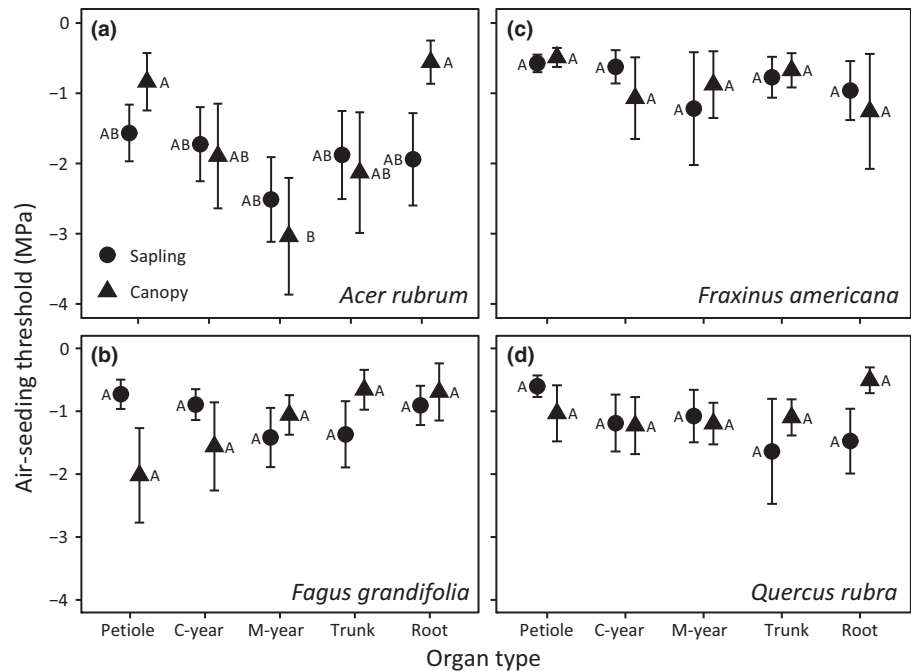


**Fig. 1** Mean air-seeding threshold (MPa) by organ type and size class for (a) *Acer rubrum*, (b) *Fagus grandifolia*, (c) *Fraxinus americana* and (d) *Quercus rubra* measured using single-vessel air-injection. More negative values indicate higher resistance to air seeding. Symbols within each panel that do not share a letter indicate Tukey's honest significant differences at  $\alpha = 0.05$ . Error bars represent  $\pm 2$  SE of the mean. Multiyear and trunk samples only include measurements from the 2016 growth ring.  $n = 9-21$  measurements per mean. C-year, current-year stem segments; M-year, multiyear stem segments.

( $-0.7 \pm 0.2$  MPa) were less resistant than the mean value for their canopy petioles ( $-2.0 \pm 0.8$  MPa; Fig. 1b).

Despite the large sample size (166 multi-year and trunk segments), we found no evidence that air-seeding threshold changed across annual growth rings (Fig. 2a-d). The air-seeding threshold of early- vs latewood xylem vessels within an annual growth ring from trunk and multi-year stems also did not differ significantly (Fig. S3). During air-seeding measurements, > 20% of the total tested vessels in most organs had no endings, and in some cases (most often in *F. americana* and *Q. rubra*), > 100 open vessels were tested in a single sample before finding a vessel with an ending that could be used for a measurement (Fig. S4).

Vessel diameter was always smaller in petioles and current-year stems than in trunks and roots (Fig. 3a-h). However, petioles and current-year stems within *A. rubrum* (both size classes), *F. grandifolia* (saplings), *F. americana* (canopy) and *Q. rubra* (both size classes) showed no significant difference in vessel diameter, nor did roots and trunks within a species for canopy size trees of all four species, or multiyear stems and trunks for sapling size *F. americana*. Mean air-seeding threshold per organ type did not vary significantly with mean vessel-lumen diameter for any species or size class (Fig. 3a-h).

The single-vessel air-seeding threshold most closely approximated  $P_{12}$  (Fig. 4; mean difference from air-seeding threshold  $\pm$  SD =  $0.10 \pm 0.43$  MPa), whereas  $P_{25}$  (mean difference from air-seeding threshold SD =  $0.48 \pm 0.31$  MPa) and  $P_{50}$  (mean difference from air-seeding threshold SD =  $1.14 \pm 0.31$  MPa) were 4.8 and 11.5 times worse predictors than  $P_{12}$ , respectively. Safety margins were calculated from the difference between the mean air-seeding threshold (and current-year  $P_{12}$  values; Fig. 4) and the minimum water potential each organ experienced during midday in late July or early August. Comparison of predawn and

midday water potential values suggests that water potentials relaxed each day by predawn (Table S1). In all cases, roots operated within their safety margins (mean =  $+0.58$  MPa; Table 1; Fig. 5a-h), whereas petioles operated at or exceeded their safety margin (mean =  $-0.49$  MPa, Table 1; Fig. 5a-h). Additionally, *A. rubrum*, *F. grandifolia* and *Q. rubra* perennial organs operated within their safety margins, but most *F. americana* organs (other than roots and sapling multi-year stems) exceeded their safety margins in both sapling and canopy trees (Table 1; Fig. 5).

## Discussion

### Single-vessel air-seeding thresholds and vulnerability segmentation

Collectively, these data show that only canopy height *Acer rubrum* trees (diffuse-porous) have different air-seeding thresholds in different organ types (Fig. 1). We also found that most organ types operated well within their hydraulic safety margins even during an episodic drought (Table 1; Fig. 5). It is important to note, as discussed below, that our safety margin estimates based on single-vessel air-seeding thresholds are more conservative than those calculated from percentage loss of conductivity (PLC) curves using the water potential where 50% of hydraulic conductivity is lost ( $P_{50}$ ) to calculate the safety margin (Choat *et al.*, 2012; Wheeler *et al.*, 2013; Johnson *et al.*, 2016). Here, mean single vessel air-seeding thresholds more closely align with the initial inflection point on the vulnerability curves for these species (i.e.  $P_{12}$ , the 'air-entry point'; Fig. 4). Therefore, the risk of the air-seeding threshold being surpassed in an individual vessel may be more than the risk of an entire vessel network reaching  $P_{50}$ . Furthermore, this interpretation is formulated in isolation from other traits that would influence the spread of embolism,

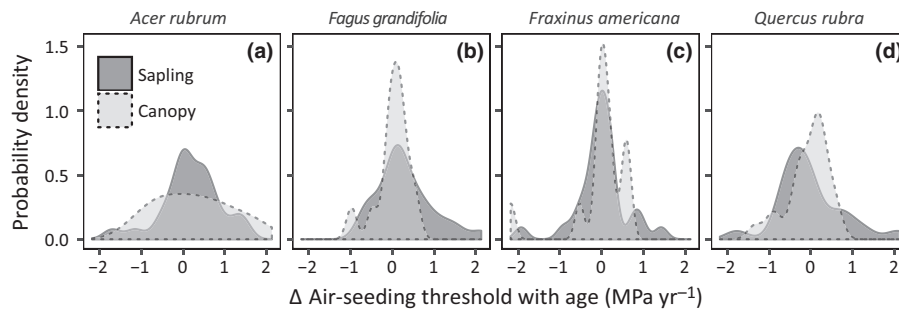


**Fig. 2** Probability density plot of the distribution of slopes of single-vessel air-seeding threshold change with vessel age by species and size class for sapling and canopy sized trees of (a) *Acer rubrum*, (b) *Fagus grandifolia*, (c) *Fraxinus americana* and (d) *Quercus rubra*. A regression between xylem age and air-seeding threshold (MPa) was calculated for each unique sample of multi-year stems and trunks containing measurements in 2016, 2015 and 2014 rings (ages 0, 1 and 2 yr; 166 segments total). Positive slopes indicate that resistance to air-seeding became less negative (also known as resistance decayed) over time. Air-seeding threshold did not consistently change with xylem age for any species or size class.

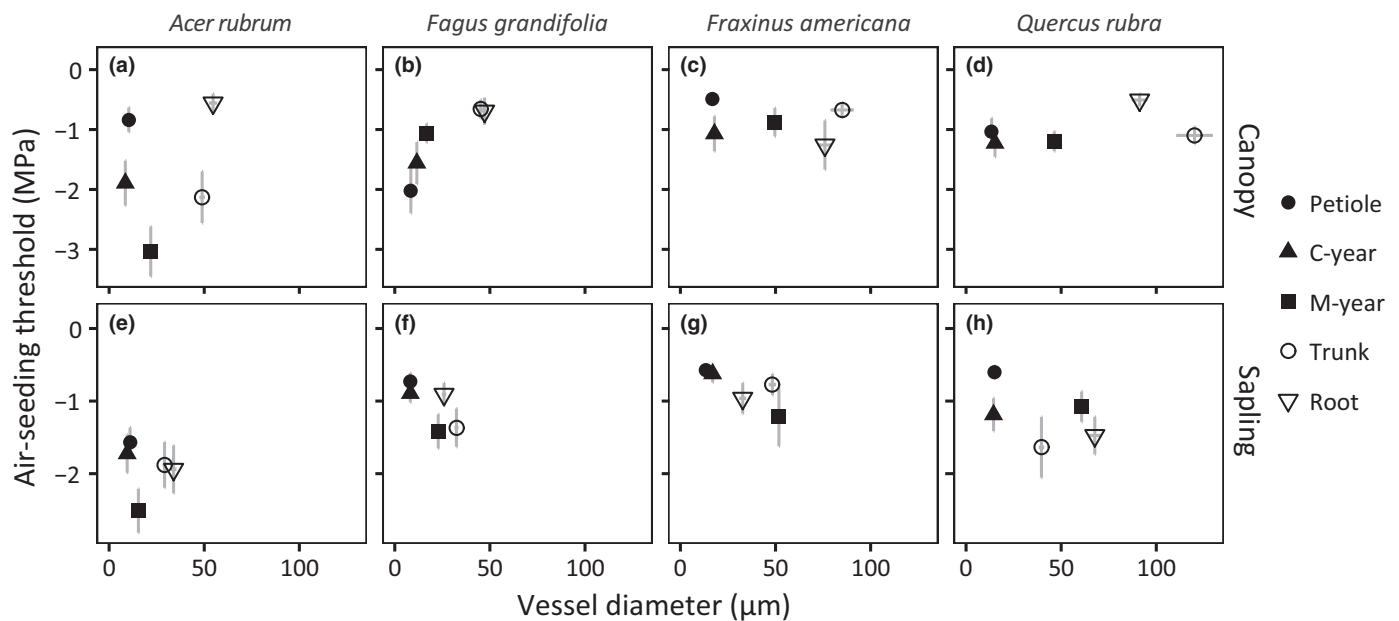


**Fig. 3** Mean single-vessel air-seeding threshold (as in Fig. 1) as a function of mean vessel diameter (error bars are  $\pm 1$  SE) for sapling and canopy-sized trees of (a, e) *Acer rubrum*, (b, f) *Fagus grandifolia*, (c, g) *Fraxinus americana* and (d, h) *Quercus rubra*. Single major axis regressions were not significant when accounting for multiple tests (Bonferroni corrected  $\alpha = 0.00625$ ). On average, 1082 vessels were used to calculate mean vessel area for each point (range 69–4895). C-year, current-year stem segments; M-year, multiyear stem segments.

such as xylem network organization and sectoriality (Ellmore *et al.*, 2006; Loepfe *et al.*, 2007; Schenk *et al.*, 2008; Brodersen *et al.*, 2010, 2011; Lee *et al.*, 2013). Although the single-vessel air injection method allows for direct comparisons of drought resistance at the scale of individual vessels, this method artificially exposes randomly selected pit membranes to air-seeding pressures, whereas a vessel *in situ* may not have air in an adjacent organ to facilitate the air-seeding mechanism. Thus, some vessels within an intact plant may persist as water-filled and functional well beyond the air-seeding threshold of the pit membranes as long as they are not exposed to air.

The segmentation of canopy *A. rubrum* based on single-vessel air-seeding thresholds corresponds well with a study at the same site in *Acer saccharum*, that also exhibited low variability of air-seeding threshold values within organs and some evidence of

mean differences across organs (Choat *et al.*, 2005). Therefore, vulnerability segmentation of canopy-sized trees may be a common trait among *Acer* species, which show stronger evidence for the hydraulic efficiency-safety trade-offs in xylem structure hypothesized by Baas *et al.* (2004) (Lens *et al.*, 2011; Gleason *et al.*, 2016). The vulnerability curve for *A. rubrum*, was consistent with others reported in the literature (cf. our  $P_{50}$  of  $-2.8$  MPa compared to  $-3.1$  MPa in Johnson *et al.*, 2016). Importantly, the air-seeding thresholds of *A. rubrum* approximated the air-entry point ( $P_{12}$ ) from the vulnerability curve for current-year stems (Fig. 4) and align with the  $P_{05}$ – $P_{20}$  range for vulnerability curves in other studies (Johnson *et al.*, 2011, 2016; Wheeler *et al.*, 2013). Greater resistance to air-seeding and partial support for vulnerability segmentation in *A. rubrum*, compared to the other three study species, may contribute to its status as a

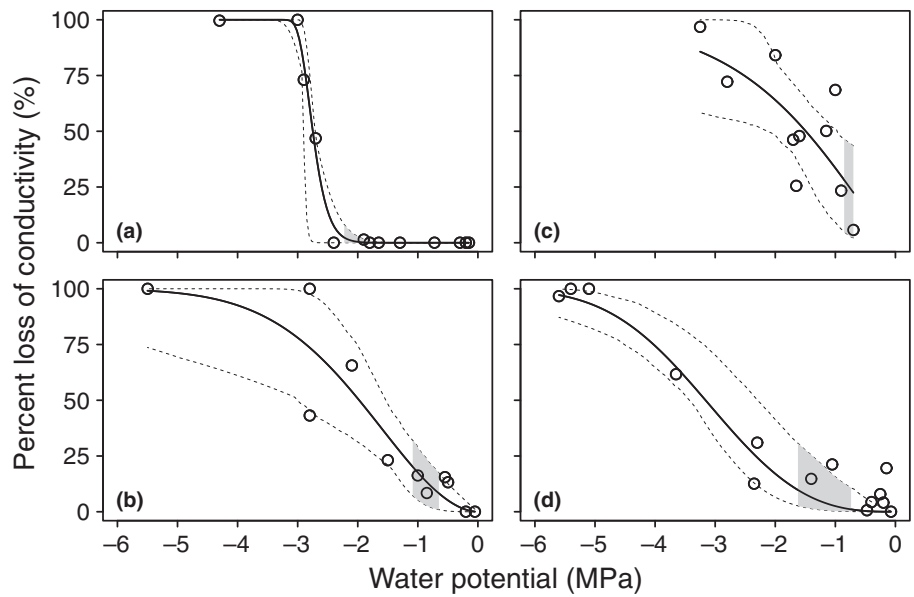


**Fig. 4** Xylem vulnerability curves for current-year stems of sapling (a) *Acer rubrum*, (b) *Fagus grandifolia*, (c) *Fraxinus americana* and (d) *Quercus rubra* generated using the benchtop dry-down method. Each point represents one measurement on one stem. Weibull fits (solid line) and 95% confidence intervals (dashed lines) are reported for each species. Shaded areas on each plot correspond to the mean air-seeding pressure ( $\pm 2$  SE) as measured using the single-vessel air-injection technique (Fig. 1).

**Table 1** Hydraulic safety margins ( $\pm$  SE) of five organ types of four northern hardwood tree species in sapling and canopy size classes

Species	Size class	Petiole	C-year	M-year	Trunk	Root
<i>Acer rubrum</i> *	Sapling	+0.21 ( $\pm$ 0.22)	+1.07 ( $\pm$ 0.27)	+1.80 ( $\pm$ 0.33)	+1.54 ( $\pm$ 0.32)	+1.71 ( $\pm$ 0.34)
<i>A. rubrum</i>	Canopy	<b>-0.71 (<math>\pm</math> 0.35)</b>	+0.56 ( $\pm$ 0.41)	+2.19 ( $\pm$ 0.42)	+1.90 ( $\pm$ 0.43)	+0.29 ( $\pm$ 0.18)
<i>Fagus grandifolia</i>	Sapling	<b>-0.52 (<math>\pm</math> 0.19)</b>	+0.13 ( $\pm$ 0.16)	+0.96 ( $\pm$ 0.24)	+0.75 ( $\pm$ 0.28)	+0.48 ( $\pm$ 0.18)
<i>F. grandifolia</i>	Canopy	+0.23 ( $\pm$ 0.39)	+0.27 ( $\pm$ 0.38)	+0.57 ( $\pm$ 0.16)	+0.24 ( $\pm$ 0.21)	+0.39 ( $\pm$ 0.25)
<i>Fraxinus americana</i>	Sapling	<b>-0.53 (<math>\pm</math> 0.15)</b>	<b>-0.52 (<math>\pm</math> 0.25)</b>	+0.12 ( $\pm$ 0.47)	<b>-1.06 (<math>\pm</math> 0.24)</b>	+0.31 ( $\pm$ 0.25)
<i>F. americana</i>	Canopy	<b>-1.57 (<math>\pm</math> 0.21)</b>	<b>-1.04 (<math>\pm</math> 0.35)</b>	<b>-2.26 (<math>\pm</math> 0.36)</b>	<b>-0.28 (<math>\pm</math> 0.17)</b>	+0.53 ( $\pm$ 0.42)
<i>Quercus rubra</i>	Sapling	<b>-1.10 (<math>\pm</math> 0.27)</b>	+0.16 ( $\pm$ 0.29)	+0.56 ( $\pm$ 0.23)	+1.20 ( $\pm$ 0.42)	+0.58 ( $\pm$ 0.43)
<i>Q. rubra</i>	Canopy	+0.08 ( $\pm$ 0.27)	+0.62 ( $\pm$ 0.26)	+0.38 ( $\pm$ 0.21)	+0.85 ( $\pm$ 0.15)	+0.32 ( $\pm$ 0.11)

Safety margins (MPa) were calculated as mean midday minimum water potential (3–6 measurements) in summer 2016 minus the mean air-seeding threshold (9–21 measurements using single-vessel air-injection) of each organ type (Fig. 5). Negative safety margins bolded for emphasis and standard errors were propagated following Taylor (1997).

\*Due to data loss, *Acer rubrum* sapling water potential data were collected on a hot day in June of 2017.

C-year, current-year stem segments; M-year, multiyear stem segments.

generalist that has been increasing in dominance in eastern forests (Abrams, 1998; Fei & Steiner, 2007).

The other diffuse-porous species, *Fagus grandifolia*, showed a general (albeit nonsignificant) trend of increasing resistance to air-seeding with increasing distance from the soil in canopy trees, the opposite of what has been found for other woody angiosperms (Choat *et al.*, 2005; Johnson *et al.*, 2016) and for saplings in this study (Fig. 1b). Interestingly, organs in *F. grandifolia* canopy trees closely followed the safety margin line (Fig. 5d) and this may be related to vessel diameter tapering from roots to shoots (Fig. 3b). *Fagus grandifolia* is shade-tolerant with rapid stomatal responses times as a sapling (Woods & Turner, 1971) and may adopt a different hydraulic strategy once it reaches full sun, similar to findings for *Fagus sylvatica* (Cochard *et al.*, 1999; Noyer *et al.*, 2017). The similar air-seeding thresholds in current-year and multi-year stems also is partially supported by data from Cochard *et al.* (1999) on *F. sylvatica*, where sun-exposed current-year stem  $P_{50}$  values were not significantly different than multi-year stems.

The two ring-porous species, *Quercus rubra* and *Fraxinus americana*, showed no significant differences in air-seeding thresholds across organ types, suggesting that they employ other strategies to withstand or avoid drought. Local studies suggest that *Q. rubra* tends to have deeper root systems than *A. rubrum* that may allow access to different ground-water sources during drought (Lyford, 1980; Burns & Honkala, 1990). The  $P_{50}$  from our benchtop vulnerability curve for *Q. rubra* was 0.6 to 0.8 MPa more resistant than others reported in the literature (Cochard *et al.*, 1992; Tyree *et al.*, 1992), and the air-seeding thresholds for current-year *Q. rubra* stems align best with the  $P_{12}$  value (Fig. 4) providing additional support that the  $P_{12}$  value can be attributed to air entry into the xylem network.

We know of no reported vulnerability curves for different organs in *F. americana*; however, our benchtop vulnerability curve is consistent with Venturas *et al.* (2016) that reports 38% loss of maximum conductivity at  $-1.4$  MPa, which is within the variability around our mean of 48% loss of conductivity at the same water potential. Again, the air-seeding threshold of current-

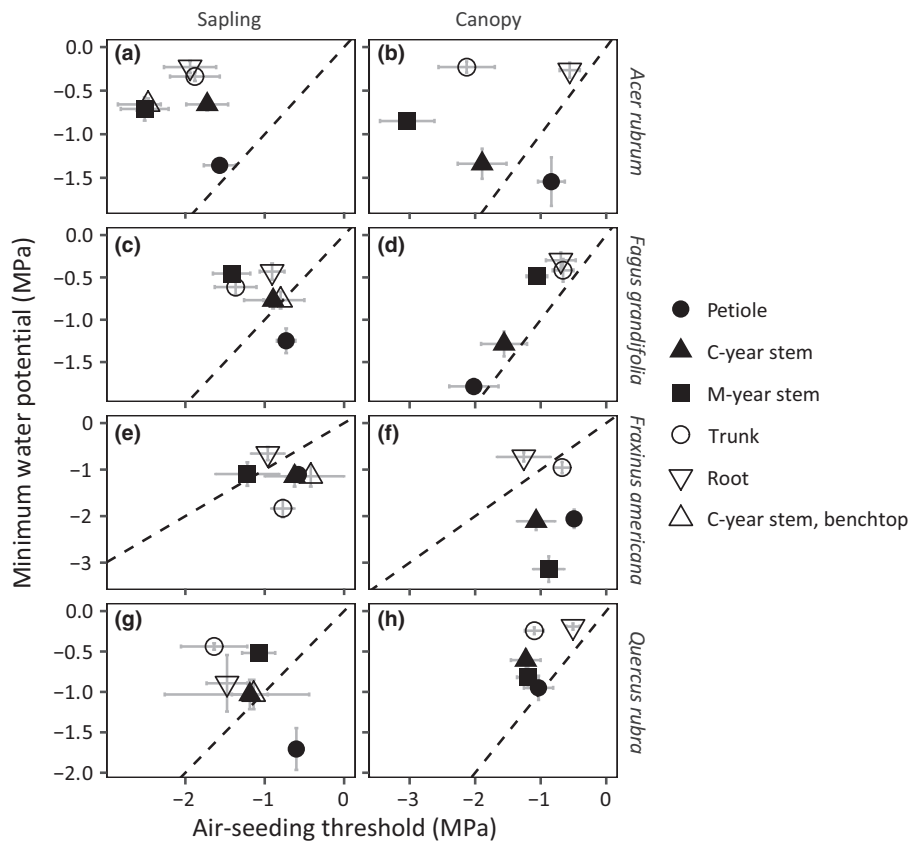


**Fig. 5** Xylem hydraulic safety margins for sapling and canopy-sized trees of (a, b) *Acer rubrum*, (c, d) *Fagus grandifolia*, (e, f) *Fraxinus americana* and (g, h) *Quercus rubra*. Safety margins (reported in Table 1) calculated as mean midday water potential minus the mean air-seeding threshold for plant organs by species and size class. Each point represents the mean air-seeding threshold measured via single-vessel air-injection and mean minimum water potential experienced at midday in July or August of 2016. Bars are SE. Upright open triangles represent safety margins calculated using  $P_{12}$  values from benchtop dry-down curves for current-year stems with 95% confidence intervals (Fig. 4). Values above the dashed 1 : 1 lines represent organs that did not experience water potentials negative enough to induce air-seeding during the growing season, whereas values falling below the 1 : 1 are for organs that would have been exposed to water potentials where air-seeding would be possible. Three water potential measurements and six air-seeding measurements were taken from each of two to three individuals for each species and size class. Due to data loss, *A. rubrum* sapling water potential data were collected on a hot day in June of 2017. C-year, current-year stem segments; M-year, multiyear stem segments.

year stems aligns best with the  $P_{12}$  value from the vulnerability curve. Our air-seeding values are slightly lower than those reported in Choat *et al.* (2004) perhaps due to individual, site or sampling differences that are not clear. We found no support for vulnerability segmentation in *F. americana*; however, there is evidence that the main stem and primary branches of *F. americana* have lower resistance to flow than lateral branches (Joyce & Steiner, 1995), suggesting that some branches could exhibit vulnerability segmentation. Furthermore, leaf xylem of *Fraxinus excelsior* experiences larger reductions in hydraulic conductance than stems leading to the possibility of vulnerability segmentation (Cochard *et al.*, 1997).

Despite the general trend of vessel diameter being smaller in petioles and current-year stems than in trunks and roots for all species, there were no consistent, statistically significant trends between mean air-seeding thresholds and mean vessel diameter, similar to Christman *et al.* (2012) but seemingly at odds with the controversial 'rare pit' hypothesis which proposes that larger vessels should be more vulnerable to embolism spread (Christman *et al.*, 2009). Furthermore, preliminary data from 2015 measured on 267 individual vessels of *Q. rubra* and *A. rubrum* saplings

showed no clear relationship between vessel diameter and air-seeding threshold (Fig. S5), suggesting that vessel diameter may not always be a good proxy for the number of intervessel connections and pits. Related to this, we also found no differences in air-seeding thresholds between earlywood and latewood vessels, contrary to expectations particularly for the ring porous species (Fig. S3; Lo Gullo *et al.*, 1995) providing further evidence that the air-seeding threshold does not vary consistently with vessel diameter or position within an annual growth ring for these species.

We found that, within an organ, resistance to air-seeding did not decline in older annual growth rings (Fig. 2) although a decline has been reported for the diffuse-porous species *A. saccharum* using single-vessel air-injection (Melcher *et al.*, 2003) and for *Populus tremuloides* using hydraulic conductivity measurements and dye staining (Sperry *et al.*, 1991). Ring-porous species in temperate regions do not typically use older rings to transport water for > 1 yr, whereas diffuse porous trees can utilize older rings for axial sap transport in conjunction with current-year xylem (cf. Umebayashi *et al.*, 2010). The trees in our study were exposed to drought and seasonal freeze-thaw cycles that are



believed to degrade pit-membrane resistance (Melcher *et al.*, 2003). However, based on the minimal impact of the severe drought on the safety margin estimates experienced by trees in our study the water deficit for the study site was unlikely to lead to significant pit membrane damage. Instead, perhaps *A. rubrum*, with relatively high resistance to air-seeding maintained that resistance for the 3 yr measured. By contrast, the other species generally had weak resistance to air-seeding, even within the current-year ring, and therefore the resistance to air-seeding would not necessarily decrease much more over time.

### Understanding the single-vessel air-seeding thresholds

The within-organ variability in air-seeding thresholds agrees with past studies using single-vessel air-injection (Melcher *et al.*, 2003; Choat *et al.*, 2005; Christman *et al.*, 2012; Johnson *et al.*, 2014; Pratt *et al.*, 2015; Venturas *et al.*, 2016) and may be driven by variability in intervessel pit area (Wheeler *et al.*, 2005) or pit membrane thickness (Li *et al.*, 2016). If individual vessel air-seeding values drive the shape of a vulnerability curve, one would expect individual vessel air-seeding values to span the entire range of the sloped portion of the vulnerability curve. Therefore, a vulnerability curve with a weak initial inflection might be predicted to have high variability in air-seeding thresholds whereas a steep-sloped vulnerability curve shape might be driven by low variability in air-seeding thresholds. Importantly, however, air spreads through a complex network of interconnected vessels of varying sizes and vulnerabilities. A network with frequent intervessel connections provides a less tortuous pathway for embolism spread; however, a few highly resistant connections (as some of our data suggest) may isolate that embolism to a discrete sector of the xylem network. Therefore, the mean air-seeding threshold of individual vessel-vessel connections within an organ would appear to approximate a value between  $P_{50}$  (assuming large amounts of network connectivity) and  $P_{12}$  (or lower; assuming less network connectivity), which our data support. Given the sigmoid shape of the vulnerability curves measured here, and those reported elsewhere in the literature for two of these species (cf. *Q. rubra* in Cochard *et al.*, 1992; *A. rubrum* in Johnson *et al.*, 2016), the variability observed in our air-seeding data is not unusual.

The single-vessel air-injection technique directly quantifies the resistance to embolism spread of individual vessels, yet there are assumptions regarding sample length that must be considered. As discussed in the methods, longer samples may result in more vessels needing to air-seed before a measurement is detected and result in artificially more-resistant air-seeding thresholds (Venturas *et al.*, 2016). Whereas vessel lengths in *A. rubrum* can be shorter than 6 cm, vessel lengths of *F. grandifolia*, *F. americana* and *Q. rubra* are typically longer than 6 cm (Zimmermann & Jeje, 1981; Zimmermann & Potter, 1982). Using a standard sample length of 6 cm, we found that usually > 25% of vessels did not have a vessel ending for a given organ suggesting that most of our measurements likely included only one vessel (Fig. S4). Furthermore, we focused on within-species comparisons to limit the confounding effect of vessel length differences between species.

### Hydraulic safety margins

Even during the third driest summer in the last 100 yr, most perennial organs of the trees studied were pushed just up to their air-seeding thresholds, but not beyond. The exception was *F. americana*, in which all organs except roots operated at or beyond their safety margin (calculated with air-seeding threshold or  $P_{12}$ ). The negative safety margins suggest lower resistance to drought at this site compared to the other species and correspond well with early leaf-drop and branch dieback in *F. americana*, noted in nearby Vermont, attributed to the 2016 drought (Vermont Department of Forests, Parks and Recreation, 2017). Interestingly, we found negative safety margins in petioles of sapling-sized *F. grandifolia* and *Q. rubra* but not canopy-size trees of the same species, suggesting, perhaps, that larger individuals of these species may have sufficient water storage to accommodate a drought of the magnitude experienced in 2016. Furthermore, our safety margins were calculated for organs that are less commonly studied but still support generally narrow margins for deciduous angiosperms (Choat *et al.*, 2012; Martin-StPaul *et al.*, 2017) except in *A. rubrum*, a species that we expect to continue expanding in eastern forests. We expect that longer or repeated droughts, however, may be a contributing factor in decline for species impacted by pests or disease.

### Conclusions

We found limited support for vulnerability segmentation of air-seeding thresholds and, except for *F. americana*, most perennial organs of trees at our study site were not pushed beyond their air-seeding thresholds, even during the third-driest growing season in recorded history. Therefore, these species may be able to tolerate the degree of drought experienced in 2016 and hydraulic failure may not be common in perennial tree organs (Cochard & Delzon, 2013). However, further research, such as experimental drought manipulation, will help to determine if these species can withstand more frequent and intense droughts (Diffenbaugh & Field, 2013). Finally, the general lack of significant differences between organ type air-seeding data for our species strongly suggests that other factors like xylem network connectivity (Ellmore *et al.*, 2006) may better explain vulnerability curve shape (Loepfe *et al.*, 2007) and calculated  $P_{50}$  values (Johnson *et al.*, 2016), because vulnerability curves are an emergent property of the entire network rather than a single network property.

### Acknowledgements


This research was supported by the National Science Foundation (IOS-1557917) and Harvard Forest Research Experience for Undergraduates program. We thank the Harvard Forest staff for facilitating this research and Ruth van Kampen and Julia Fisher for help with data collection. Sylvain Delzon and three anonymous reviewers provided feedback that improved this manuscript.

## Author contributions

B.A.H. and C.R.B. conceptualized and planned the research; J.W.W., K.S.A., N.S., B.A.H. and C.R.B. designed and conducted the research; J.W.W. analyzed the data; and J.W.W., B.A.H. and C.R.B. wrote the manuscript.

## ORCID

Jay W. Wason  <http://orcid.org/0000-0003-1338-881X>

Craig R. Brodersen  <http://orcid.org/0000-0002-0924-2570>

## References

- Abrams MD. 1998. The red maple paradox. *BioScience* 48: 355–364.
- Adams HD, Zeppel MJB, Anderegg WRL, Hartmann H, Landhäusser SM, Tissue DT, Huxman TE, Hudson PJ, Franz TE, Allen CD *et al.* 2017. A multi-species synthesis of physiological mechanisms in drought-induced tree mortality. *Nature Ecology & Evolution* 1: 1285.
- Allen CD, Macalady AK, Chenchouni H, Bachelet D, McDowell N, Venetier M, Kitzberger T, Rigling A, Breshears DD, Hogg EH *et al.* 2010. A global overview of drought and heat-induced tree mortality reveals emerging climate change risks for forests. *Forest Ecology and Management* 259: 660–684.
- Anderegg WR, Meinzer FC. 2015. Wood anatomy and plant hydraulics in a changing climate. In: Hacke U, ed. *Functional and ecological xylem anatomy*. Cham, Switzerland: Springer International Publishing, 235–253.
- Baas P, Ewers FW, Davis SD, Wheeler EA. 2004. Evolution of xylem physiology. *The Evolution of Plant Physiology* 273: 273–291.
- Bates D, Maechler M, Bolker B, Walker S, Christensen RHB, Singmann H, Dai B, Grothendieck G, Green P. 2016. *lme4: Linear Mixed-Effects Models using Eigen' and S4*. R package version: 1.1.14. [WWW document] URL <https://cran.r-project.org/web/packages/lme4/index.html>
- Bouche PS, Delzon S, Choat B, Badel E, Brodribb TJ, Burrett R, Cochard H, Charra-Vaskou K, Lavigne B, Li S *et al.* 2016. Are needles of *Pinus pinaster* more vulnerable to xylem embolism than branches? New insights from X-ray computed tomography. *Plant, Cell & Environment* 39: 860–870.
- Boyer JS. 1967. Leaf water potentials measured with a pressure chamber. *Plant Physiology* 42: 133–137.
- Brodersen CR. 2016. Finding support for theoretical tradeoffs in xylem structure and function. *New Phytologist* 209: 8–10.
- Brodersen CR, Lee EF, Choat B, Jansen S, Phillips RJ, Shackel KA, McElrone AJ, Matthews MA. 2011. Automated analysis of three-dimensional xylem networks using high-resolution computed tomography. *New Phytologist* 191: 1168–1179.
- Brodersen CR, McElrone AJ, Choat B, Matthews MA, Shackel KA. 2010. The dynamics of embolism repair in xylem: *in vivo* visualizations using high-resolution computed tomography. *Plant Physiology* 154: 1088–1095.
- Brodribb TJ, Cochard H. 2009. Hydraulic failure defines the recovery and point of death in water-stressed conifers. *Plant Physiology* 149: 575–584.
- Brown RW, Bartos DL. 1982. A calibration model for screen-caged Peltier thermocouple psychrometers. *NASA STI/Recon Technical Report N83*: 155.
- Bucci SJ, Scholz FG, Campanello PI, Montti L, Jimenez-Castillo M, Rockwell FA, Manna LL, Guerra P, Bernal PL, Troncoso O *et al.* 2012. Hydraulic differences along the water transport system of South American Nothofagus species: do leaves protect the stem functionality? *Tree Physiology* 32: 880–893.
- Burns RM, Honkala BH. 1990. Silvics of North America. Agriculture Handbook 654, U.S. Dept of Agriculture, Forest Service, Washington, DC, USA.
- Charrier G, Torres-Ruiz JM, Badel E, Burrett R, Choat B, Cochard H, Delmas CE, Domec J-C, Jansen S, King A *et al.* 2016. Evidence for hydraulic vulnerability segmentation and lack of xylem refilling under tension. *Plant Physiology* 172: 1657–1668.
- Choat B, Drayton WM, Brodersen C, Matthews MA, Shackel KA, Wada H, McElrone AJ. 2010. Measurement of vulnerability to water stress-induced cavitation in grapevine: a comparison of four techniques applied to a long-veined species. *Plant, Cell & Environment* 33: 1502–1512.
- Choat B, Jansen S, Brodribb TJ, Cochard H, Delzon S, Bhaskar R, Bucci SJ, Feild TS, Gleason SM, Hacke UG *et al.* 2012. Global convergence in the vulnerability of forests to drought. *Nature* 491: 752–755.
- Choat B, Jansen S, Zwieniecki MA, Smets E, Holbrook NM. 2004. Changes in pit membrane porosity due to deflection and stretching: the role of vested pits. *Journal of Experimental Botany* 55: 1569–1575.
- Choat B, Lahr EC, Melcher PJ, Zwieniecki MA, Holbrook NM. 2005. The spatial pattern of air seeding thresholds in mature sugar maple trees. *Plant, Cell & Environment* 28: 1082–1089.
- Christman MA, Sperry JS, Adler FR. 2009. Testing the 'rare pit' hypothesis for xylem cavitation resistance in three species of *Acer*. *New Phytologist* 182: 664–674.
- Christman MA, Sperry JS, Smith DD. 2012. Rare pits, large vessels and extreme vulnerability to cavitation in a ring-porous tree species. *New Phytologist* 193: 713–720.
- Cochard H, Bréda N, Granier A, Aussenac G. 1992. Vulnerability to air embolism of three European oak species (*Quercus petraea* (Matt) Liebl, *Q pubescens* Willd., *Q robur* L.). *Annales des Sciences Forestières* 49: 225–233.
- Cochard H, Delzon S. 2013. Hydraulic failure and repair are not routine in trees. *Annals of Forest Science* 70: 659–661.
- Cochard H, Lemoine D, Dreyer E. 1999. The effects of acclimation to sunlight on the xylem vulnerability to embolism in *Fagus sylvatica* L. *Plant, Cell & Environment* 22: 101–108.
- Cochard H, Peiffer M, Le Gall K, André G. 1997. Developmental control of xylem hydraulic resistances and vulnerability to embolism in *Fraxinus excelsior* L.: impacts on water relations. *Journal of Experimental Botany* 48: 655–663.
- Delzon S, Cochard H. 2014. Recent advances in tree hydraulics highlight the ecological significance of the hydraulic safety margin. *New Phytologist* 203: 355–358.
- Diffenbaugh NS, Field CB. 2013. Changes in ecologically critical terrestrial climate conditions. *Science* 341: 486–492.
- Dixon HH, Joly J. 1895. On the ascent of sap. *Philosophical Transactions of the Royal Society B* 186: 563–576.
- Duursma R, Choat B. 2017. fitplc – an R package to fit hydraulic vulnerability curves. *Journal of Plant Hydraulics* 4: e-002.
- Ellmore GS, Zanne AE, Orians CM. 2006. Comparative sectoriality in temperate hardwoods: hydraulics and xylem anatomy. *Botanical Journal of the Linnean Society* 150: 61–71.
- Espino S, Schenk HJ. 2011. Mind the bubbles: achieving stable measurements of maximum hydraulic conductivity through woody plant samples. *Journal of Experimental Botany* 62: 1119–1132.
- Fei S, Steiner KC. 2007. Evidence for increasing red maple abundance in the Eastern United States. *Forest Science* 53: 473–477.
- Gärtner H, Lucchinetti S, Schweingruber FH. 2014. New perspectives for wood anatomical analysis in dendrosciences: the GSL1-microtome. *Dendrochronologia* 32: 47–51.
- Gleason SM, Westoby M, Jansen S, Choat B, Hacke UG, Pratt RB, Bhaskar R, Brodribb TJ, Bucci SJ, Cao K-F *et al.* 2016. Weak tradeoff between xylem safety and xylem-specific hydraulic efficiency across the world's woody plant species. *New Phytologist* 209: 123–136.
- Hacke U, Sauter JJ. 1996. Drought-induced xylem dysfunction in petioles, branches, and roots of *Populus balsamifera* L. and *Alnus glutinosa* (L.) Gaertn. *Plant Physiology* 111: 413–417.
- Hao G-Y, Wheeler JK, Holbrook NM, Goldstein G. 2013. Investigating xylem embolism formation, refilling and water storage in tree trunks using frequency domain reflectometry. *Journal of Experimental Botany* 64: 2321–2332.
- Hochberg U, Albuquerque C, Rachmilevitch S, Cochard H, David-Schwartz R, Brodersen CR, McElrone A, Windt CW. 2016. Grapevine petioles are more sensitive to drought induced embolism than stems: evidence from *in vivo* MRI and microcomputed tomography observations of hydraulic vulnerability segmentation. *Plant, Cell & Environment* 39: 1886–1894.
- Jansen S, Choat B, Pletsers A. 2009. Morphological variation of intervessel pit membranes and implications to xylem function in angiosperms. *American Journal of Botany* 96: 409–419.

- Johnson DM, Brodersen CR, Reed M, Domec J-C, Jackson RB. 2014. Contrasting hydraulic architecture and function in deep and shallow roots of tree species from a semi-arid habitat. *Annals of Botany* 113: 617–627.
- Johnson DM, McCulloh KA, Meinzer FC, Woodruff DR, Eissenstat DM. 2011. Hydraulic patterns and safety margins, from stem to stomata, in three eastern US tree species. *Tree Physiology* 31: 659–668.
- Johnson DM, Wortemann R, McCulloh KA, Jordan-Meille L, Ward E, Warren JM, Palmroth S, Domec J-C. 2016. A test of the hydraulic vulnerability segmentation hypothesis in angiosperm and conifer tree species. *Tree Physiology* 36: 983–993.
- Joyce BJ, Steiner KC. 1995. Systematic variation in xylem hydraulic capacity within the crown of white ash (*Fraxinus americana*). *Tree Physiology* 15: 649–656.
- Lee EF, Matthews MA, McElrone AJ, Phillips RJ, Shackel KA, Brodersen CR. 2013. Analysis of HRCT-derived xylem network reveals reverse flow in some vessels. *Journal of Theoretical Biology* 333: 146–155.
- Lens F, Sperry JS, Christman MA, Choat B, Rabaey D, Jansen S. 2011. Testing hypotheses that link wood anatomy to cavitation resistance and hydraulic conductivity in the genus *Acer*. *New Phytologist* 190: 709–723.
- Li S, Klepsch M, Jansen S, Schmitt M, Lens F, Karimi Z, Schuldt B, Espino S, Schenk HJ. 2016. Intervessel pit membrane thickness as a key determinant of embolism resistance in angiosperm xylem. *IAWA Journal* 37: 152–171.
- Lo Gullo MA, Salleo S, Piaceri EC, Rosso R. 1995. Relations between vulnerability to xylem embolism and xylem conduit dimensions in young trees of *Quercus corris*. *Plant, Cell & Environment* 18: 661–669.
- Loepfe L, Martinez-Vilalta J, Pinol J, Mencuccini M. 2007. The relevance of xylem network structure for plant hydraulic efficiency and safety. *Journal of Theoretical Biology* 247: 788–803.
- Lyford WH. 1980. *Development of the root system of northern red oak* (*Quercus rubra* L.). Petersham, MA, USA: Harvard University, Harvard Forest.
- Martin-StPaul N, Delzon S, Cochard H. 2017. Plant resistance to drought depends on timely stomatal closure. *Ecology Letters* 20: 1437–1447.
- Meinzer FC, Johnson DM, Lachenbruch B, McCulloh KA, Woodruff DR. 2009. Xylem hydraulic safety margins in woody plants: coordination of stomatal control of xylem tension with hydraulic capacitance. *Functional Ecology* 23: 922–930.
- Meinzer FC, McCulloh KA. 2013. Xylem recovery from drought-induced embolism: where is the hydraulic point of no return? *Tree Physiology* 33: 331–334.
- Melcher PJ, Zwieniecki MA, Holbrook NM. 2003. Vulnerability of xylem vessels to cavitation in sugar maple. Scaling from individual vessels to whole branches. *Plant Physiology* 131: 1775–1780.
- Mencuccini M, Martinez-Vilalta J, Piñol J, Loepfe L, Burnat M, Alvarez X, Camacho J, Gil D. 2010. A quantitative and statistically robust method for the determination of xylem conduit spatial distribution. *American Journal of Botany* 97: 1247–1259.
- Noyer E, Lachenbruch B, Dlouhá J, Collet C, Ruelle J, Ningre F, Fournier M. 2017. Xylem traits in European beech (*Fagus sylvatica* L.) display a large plasticity in response to canopy release. *Annals of Forest Science* 74: 46.
- Pratt RB, MacKinnon ED, Venturas MD, Crous CJ, Jacobsen AL. 2015. Root resistance to cavitation is accurately measured using a centrifuge technique. *Tree Physiology* 35: 185–196.
- R Core Team. 2015. *R: a language and environment for statistical computing*. Vienna, Austria: R Foundation for Statistical Computing.
- Rossi S, Anfodillo T, Menardi R. 2006. Trephor: a new tool for sampling microcores from tree stems. *IAWA Journal* 27: 89–97.
- Schenk HJ, Espino S, Goedhart CM, Nordenstahl M, Cabrera HIM, Jones CS. 2008. Hydraulic integration and shrub growth form linked across continental aridity gradients. *Proceedings of the National Academy of Sciences, USA* 105: 11 248–11 253.
- Scholander PF, Hammel HT, Bradstreet ED, Hemmingsen EA. 1965. Sap pressure in vascular plants. *Science* 148: 339–346.
- Skelton RP, Brodribb TJ, Choat B. 2017. Casting light on xylem vulnerability in an herbaceous species reveals a lack of segmentation. *New Phytologist* 214: 561–569.
- Sperry JS, Donnelly JR, Tyree MT. 1988. A method for measuring hydraulic conductivity and embolism in xylem. *Plant, Cell & Environment* 11: 35–40.
- Sperry JS, Perry AH, Sullivan JEM. 1991. Pit membrane degradation and air-embolism formation in ageing xylem vessels of *Populus tremuloides* Michx. *Journal of Experimental Botany* 42: 1399–1406.
- Taylor JR. 1997. *An introduction to error analysis: the study of uncertainties in physical measurements*. Sausalito, CA, USA: University Science Books.
- Torres-Ruiz JM, Jansen S, Choat B, McElrone AJ, Cochard H, Brodribb TJ, Badel E, Burlett R, Bouche PS, Brodersen CR *et al.* 2015. Direct X-ray microtomography observation confirms the induction of embolism upon xylem cutting under tension. *Plant Physiology* 167: 40–43.
- Tsuda M, Tyree MT. 1997. Whole-plant hydraulic resistance and vulnerability segmentation in *Acer saccharinum*. *Tree Physiology* 17: 351–357.
- Tyree MT, Alexander J, Machado J-L. 1992. Loss of hydraulic conductivity due to water stress in intact juveniles of *Quercus rubra* and *Populus deltoides*. *Tree Physiology* 10: 411–415.
- Tyree MT, Cochard H, Cruiziat P, Sinclair B, Ameglio T. 1993. Drought-induced leaf shedding in walnut: evidence for vulnerability segmentation. *Plant, Cell & Environment* 16: 879–882.
- Tyree MT, Sperry JS. 1989. Vulnerability of xylem to cavitation and embolism. *Annual Review of Plant Biology* 40: 19–36.
- Tyree MT, Zimmermann MH. 2002. *Xylem structure and the ascent of sap*. Berlin: Springer.
- Umebayashi T, Utsumi Y, Koga S, Inoue S, Matsumura J, Oda K, Fujikawa S, Arakawa K, Otsuki K. 2010. Xylem water-conducting patterns of 34 broadleaved evergreen trees in southern Japan. *Trees* 24: 571–583.
- Urli M, Porté AJ, Cochard H, Guengant Y, Burlett R, Delzon S. 2013. Xylem embolism threshold for catastrophic hydraulic failure in angiosperm trees. *Tree Physiology* 33: 672–683.
- Venturas MD, Rodríguez-Zaccaro FD, Percolla MI, Crous CJ, Jacobsen AL, Pratt RB. 2016. Single vessel air injection estimates of xylem resistance to cavitation are affected by vessel network characteristics and sample length. *Tree Physiology* 36: 1247–1259.
- Vermont Department of Forests, Parks and Recreation. 2017. *Vermont Forest Health Highlights*. Forest Health Report 2017-12. [WWW document] URL [http://fpr.vermont.gov/sites/fpr/files/Forest\\_and\\_Forestry/Forest\\_Health/Library/2017%20VT%20Forest%20Health%20Highlights.pdf](http://fpr.vermont.gov/sites/fpr/files/Forest_and_Forestry/Forest_Health/Library/2017%20VT%20Forest%20Health%20Highlights.pdf). [accessed December 2017].
- Warton D, Duursma R, Falster D, Taskinen S. 2014. *smatr: (Standardised) Major Axis Estimation and Testing Routines*. R package version: 3.4.3. [WWW document] URL <https://cran.r-project.org/web/packages/smatr/index.html>
- van der Werf GW, Sass-Klaassen UGW, Mohren GMJ. 2007. The impact of the 2003 summer drought on the intra-annual growth pattern of beech (*Fagus sylvatica* L.) and oak (*Quercus robur* L.) on a dry site in the Netherlands. *Dendrochronologia* 25: 103–112.
- Wheeler JK, Huggert BA, Tofte AN, Rockwell FE, Holbrook NM. 2013. Cutting xylem under tension or supersaturated with gas can generate PLC and the appearance of rapid recovery from embolism: sampling induced embolism. *Plant, Cell & Environment* 36: 1938–1949.
- Wheeler JK, Sperry JS, Hacke UG, Hoang N. 2005. Inter-vessel pitting and cavitation in woody Rosaceae and other vesselless plants: a basis for a safety versus efficiency trade-off in xylem transport. *Plant, Cell & Environment* 28: 800–812.
- Wickham H, Chang W. 2016. *ggplot2: Create elegant data visualisations using the grammar of graphics*. R package version: 2.2.1. [WWW document] URL <https://cran.r-project.org/web/packages/ggplot2/index.html>
- Woods DB, Turner NC. 1971. Stomatal response to changing light by four tree species of varying shade tolerance. *New Phytologist* 70: 77–84.
- Zhang Y, Klepsch M, Jansen S. 2017. Bordered pits in xylem of vesselless angiosperms and their possible misinterpretation as perforation plates. *Plant, Cell & Environment* 40: 2133–2146.
- Zhu S-D, Liu H, Xu Q-Y, Cao K-F, Ye Q. 2016. Are leaves more vulnerable to cavitation than branches? *Functional Ecology* 30: 1740–1744.
- Zimmermann MH. 1983. *Xylem structure and the ascent of sap*. Berlin: Springer.
- Zimmermann MH, Jeje AA. 1981. Vessel-length distribution in stems of some American woody plants. *Canadian Journal of Botany* 59: 1882–1892.
- Zimmermann MH, Potter D. 1982. Vessel-length distribution in branches, stem and roots of *Acer rubrum*. *IAWA Bulletin* 3: 103–109.

## Supporting Information

Additional Supporting Information may be found online in the Supporting Information tab for this article:

**Fig. S1** Palmer Drought Severity Index for study area.

**Fig. S2** Comparison of thermocouple psychrometer and pressure chamber water potentials.

**Fig. S3** Earlywood and latewood air-seeding thresholds.

**Fig. S4** Proportion of open vessels encountered during sampling.

**Fig. S5** Relationship between vessel diameter and air-seeding threshold.

**Table S1** Predawn and midday leaf water potentials

Please note: Wiley Blackwell are not responsible for the content or functionality of any Supporting Information supplied by the authors. Any queries (other than missing material) should be directed to the *New Phytologist* Central Office.



## About *New Phytologist*

- *New Phytologist* is an electronic (online-only) journal owned by the New Phytologist Trust, a **not-for-profit organization** dedicated to the promotion of plant science, facilitating projects from symposia to free access for our Tansley reviews and Tansley insights.
- Regular papers, Letters, Research reviews, Rapid reports and both Modelling/Theory and Methods papers are encouraged. We are committed to rapid processing, from online submission through to publication 'as ready' via *Early View* – our average time to decision is <26 days. There are **no page or colour charges** and a PDF version will be provided for each article.
- The journal is available online at Wiley Online Library. Visit **www.newphytologist.com** to search the articles and register for table of contents email alerts.
- If you have any questions, do get in touch with Central Office (np-centraloffice@lancaster.ac.uk) or, if it is more convenient, our USA Office (np-usaoffice@lancaster.ac.uk)
- For submission instructions, subscription and all the latest information visit **www.newphytologist.com**